Synthesis of Kaolin Loaded Ag and Ni Nanocomposites and Their Applicability for the Removal of Malachite Green Oxalate Dye

Hajira, Tahir*[+]***; Atika, Saud; Muhammad, Saad.***
Department of Chemistry, University of Karachi, Karachi, PAKISTAN

ABSTRACT: *The present study focuses on the synthesis of Kaolin loaded Silver (Ag-KNC) and Nickel (Ni-KNC) nanocomposites by co-precipitation method. The surface morphology of them was determined by SEM technique while chemical composition was determined by FT-IR technique. The removal of Malachite Green Oxalate (MGO) was preceded by the adsorption method using (Ag-KNC) and (Ni-KNC). The adsorption models like Freundlich, Langmuir, and D-R (Dubinin-Radushkevich) was utilized to figure out the applicability of the tactic. Moreover, the pH at the point of zero charge (pH_{pzc}) was determined to find surface neutrality. The effect of electrolyte (KCl) on the removal efficacy of MGO was additionally investigated. Furthermore, the ionic strength and thickness of Electrical Double Layer (EDL) were also determined. Thermodynamic parameters like free energy (ΔG^o), entropy (ΔS^o) and enthalpy (ΔH^o), of the system, was also investigated. The adsorption Kinetic was resolute by Intra Particle Diffusion (IPD) and Boyd's models. Moreover, the adsorption efficacy was effectuality was ascertained to be 88% for (Kaolin), 97% for (Ag-KNC) and 95% for (Ni-KNC) systems.*

KEYWORDS: *Nanocomposites; Adsorption models; pH_{pzc}; EDL; FT-IR; SEM.*

INTRODUCTION

The strategies for the fabrication of nanocomposites have fundamental importance within the advancement of nanotechnology [1]. The size of nanocomposites reduced by nanofabrication process and it provides an improved surface area of materials [2]. The nanocomposites synthesized by bottom-up approach receive attention attributable to their intrinsic size-dependent properties. Furthermore, they possess unique properties compeered to conventional methods. They have the ability to overcome limitations of micro-composites and monolithic [3]. Moreover throughout this context, the surface area/volume magnitude relation of nanocomposites is crucial to recognize the structural properties [4].

In addition nanocomposites together with nanoparticles and nanofillers are considering metal oxide, chemical-based nanocomposites, and carbon nanotubes. The fullerene-based nanocomposites have low mass and show tremendous mechanical and thermal properties [5-9]. Apart from their application, they show glorious removal efficiencies for numerous significant metals and dyes from wastewater [10].

The metal nanoparticles (NPs) have remarkable physical and chemical properties proven from worldwide

***** *To whom correspondence should be addressed.*
+ E-mail: hajirat@uok.edu.pk
1021-9986/2018/2/11-22 *12/$/6.02*

investigation [11]. The Silver nanoparticles (Ag-NPs) have a variety of superior properties and are widely utilized in several fields and widely used as antibacterial agents, catalysts, photocatalysts, photosensitive components and surface enhancer [12-17].

The Nickle nanoparticles (Ni-NPs) even have wide application spanning over numerous fields including catalytic, conducting and magnetic properties. They reduce dyes in a very short span of time [18]. Additionally, they wore within the hydrogenation of Furfural (2-furaldehyde) [19]. Moreover, they have the property of controlling carbon deposition and deactivations of active sites. The nanostructured electrochemical capacitors were synthesized and apply for the waste minimization by electro-coagulation method [20]. The synthesis of Ni-NPs in the binary compound is enticing attributable to their existence and promising physical and chemical properties.

Dyes are considerably utilized in numerous industries. Customarily they are toxic and some of them are mutagenic and carcinogenic [21]. Moreover, the effluent from different industrial units causes contamination of water bodies [22]. They not only pollute the water resources but their persistence disturbs the photosynthetic activity[23]. The adsorbents like activated carbon [24] chitosan [25] fly ash [26] are widely employed by scientists as well as showing removal efficiencies for the minimization of wastewater.

Various techniques including biodegradation, photocatalytic degradation, solvent extraction, and chemical oxidation have been adopted by numerous researchers for the remediation of dyes wastewater. In the present study Kaolin ($Al_2O_3.2SiO_2$) was used as a natural adsorbent having plate-like lamellar shape. The morphological structure represents that the silicate (Si_2O_5) sheets were bonded to aluminum hydroxide ($Al_2(OH)_4$)[27-30]. They also have many biomedical applications.

The present study represents a unified approach to synthesize nanocomposites with enhanced surface properties. The results revealed that the synthesized nanocomposites show excellent potential for the removal of toxic dyes and remediation of wastewater.

EXPERIMENTAL SECTION

The naturally occurring mineral Kaolin ($Al_2O_3.2SiO_2$) was provided by Sigma. Whereas absolute Ethanol (C_2H_5OH), Hydrochloric Acid (HCl) and Nickel (II) chloride hexahydrate ($NiCl_2.6H_2O$) were supplied by BDH laboratories. Sodium Hydroxide (NaOH), Sodium carbonate anhydrous (Na_2CO_3) and Silver Nitrate ($AgNO_3$) were provided by AVON-CHEM laboratories. Malachite green Oxalate (MGO) (C.I. # 42000) was used with relative molecular mass 927.02gm/mol and molar extinction coefficient 148900 $M^{-1}cm^{-1}$[31] .

Nanocomposites synthesis

The (Ag-KNC) nanocomposites were synthesized by co-precipitation method. For the synthesis of them about 2.0 g $Al_2O_3.2SiO_2$ was baked at 120°C for two hours. After that, it was mixed with 200 mL C_2H_5OH under constant stirring at 120 rpm for 2 hours in a shaking incubator. Succeeding to that $Al_2O_3.2SiO_2$ was well dispersed and 3mL NaOH (5%) was added in the reaction mixture under constant stirred conditions and after that, it was left for 24 hours at room temperature. Subsequently, 30 mL of $AgNO_3$ (7.6 g/L in C_2H_5OH) was added in the respective content at the rate of 0.5 mL/min. Later the precipitate of (Ag-KNC) was filtered by several items of washing with deionized water and dried at room temperature [32].

Moreover, the synthesis of (Ni-KNC) nanocomposites is mainly two steps process. Initially, the kaolin/$Na_2Ni_3(CO_3)_4\cdot(H_2O)_3$ composite was prepared by the reaction of $NiCl_2$ and Na_2CO_3 in the presence of $Al_2O_3.2SiO_2$. After that precursor was oven dried at 100 °C. In the next step, the $Al_2O_3.2SiO_2/Na_2Ni_3(CO_3)_4\cdot(H_2O)_3$ precursor was calcinated at 600 °C to transformed into the (Ni-KNC) by its 1.0 h [33].

Characterization of nanocomposites

The optical and morphological properties of (Ag-KNC) and (Ni-KNC) were determined by using UV-Visible spectrophotometer (T80 UV/VIS spectrometer. PG instrument Limited, UK) at 200-800nm range. The Fourier Transform InfraRed (FT-IR) spectroscopy (IR-Prestige 21-Shimadzu) from 4000-400cm^{-1} wavelength range, and Scanning Electron Microscopy (JEOL; Japan, JSM 5910) at 15KV.

Protocol of adsorption studies

The adsorption experiments were preceded under the effect of certain adsorption conditions like the dosage of

nanocomposites, pH, shaking time, pH, at the point of zero charge (pH_{ZPC}) and ionic strength effect. The experiments were preceded using 500 mg/L solution of MGO dye.

Adsorption isotherms

The adsorption isotherms including Freundlich, Langmuir and Dubinin Radushkevich (D-R) were elicited for Kaolin, (Ag-KNC) and (Ni-KNC) systems under the effect of optimized parameters within the temperatures 298K to 313K.

RESULT AND DISCUSSION

Characterization of Nanocomposites

FTIR Analysis

FTIR Spectra of Kaolin, Ag-KNC, and Ni-KNC before and after adsorption are shown in Fig. 1. The main peaks appeared in the infrared region reflects Al-OH, Al-O and Si-O functional groups in the high frequency stretching and low frequency bending modes. It was observed that bands appeared are close to those obtained for theoretical kaolinite. Moreover, the peaks for theoretical kaolinite, represent pure kaolinite with the chemical formula $Al_2Si_2O_5(OH)_4$, and exhibited OH stretching bands at3620, 3621, 3694 cm^{-1}. The bands appeared at 3433–3693cm^{-1} corresponds to the stretching mode vibration of the OH group; verify the presence of OH groups attached to the octahedral layer of $Al_2O_3.2SiO_2$. The presence of peaks at 1650 cm^{-1}, 1031 cm^{-1}, and 538 cm^{-1} represents the Si–O stretching band. The Si–O–Si asymmetric stretching band and the Si–O–Al bands were observed in all sets. The peaks appeared at 110cm^{-1}, 475cm^{-1} indicates the presence of Ag and Ni particles respectively for both the system before and after the adsorption onto the $Al_2O_3.2SiO_2$ before and after adsorption of Ag-KNC and Ni-KNC [34].

Scanning Electron Microscopy (SEM) analysis

It was observed that the sizes varied between 100-50nm for both Ag-KNC and Ni-KNC nanocomposites that seem brighter surface and supported by the darker plane of $Al_2O_3.2SiO_2$ as shown in Fig. 2 (a-d). It was observed that the average particle size ranges from 50.00nm to 100 nm.

The empty sites appeared on the surface of Ag-KNC and Ni-KNC provides active sites for the adsorption of dye molecules. After adsorption empty spaces were crowded

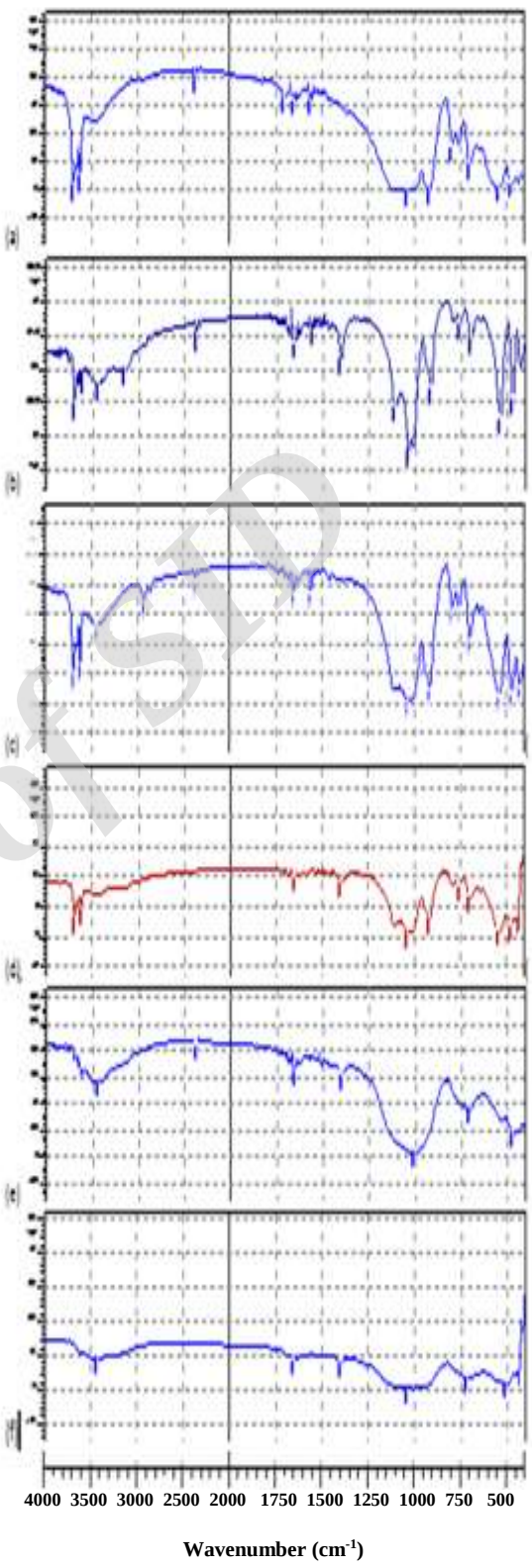

Fig. 1: FT-IR Spectra of Kaolin, Ag-KNC and Ni-KNC nanocomposites before and after adsorption of MGO.

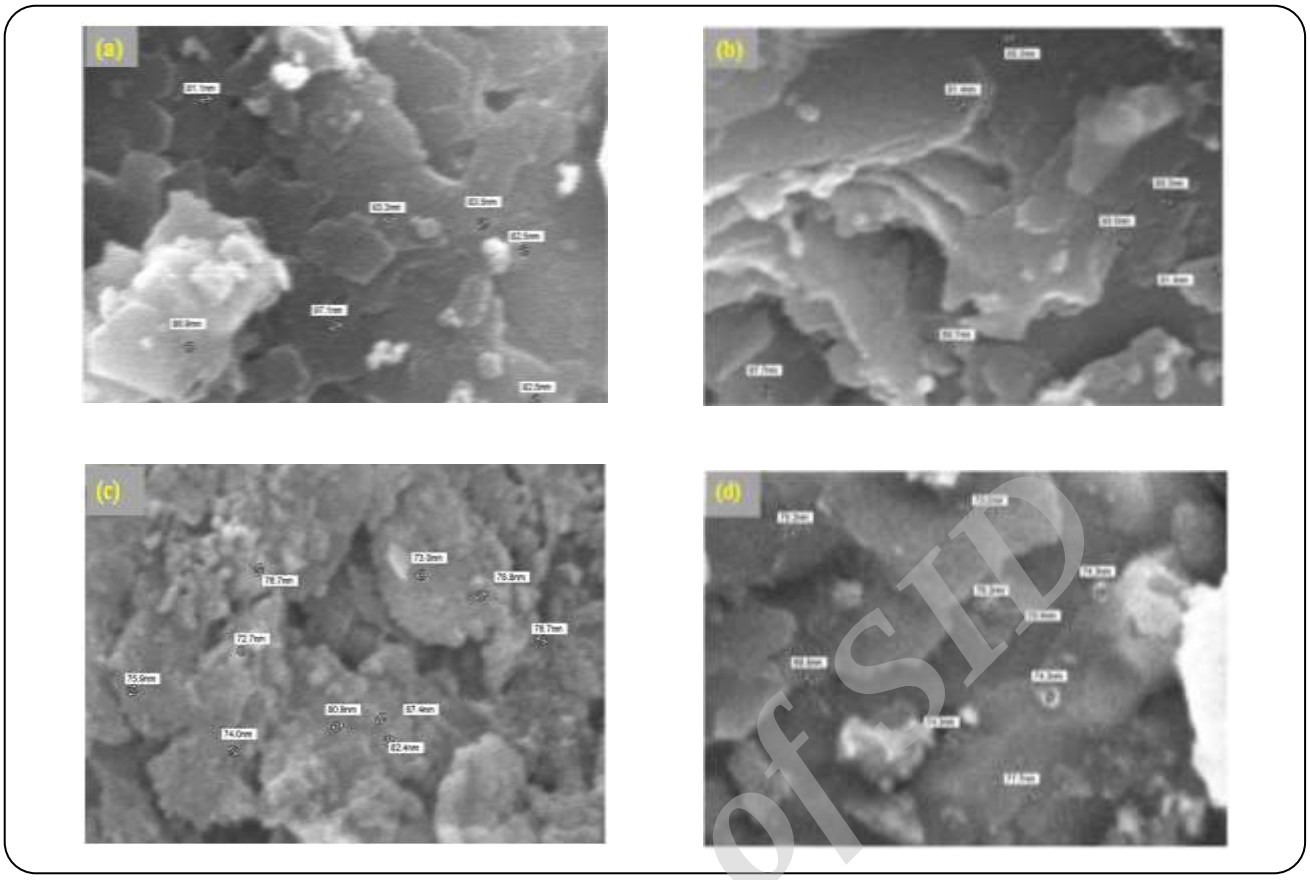

Fig. 2: (a) SEM image of Ag-KNC before Adsorption, (b) Ag-KNC after Adsorption, (c) Ni-KNC before Adsorption, (d) Ni-KNC after Adsorption.

by dye molecules that were adsorbed on the surface of Ag-*KNC and Ni-KNC.*

Batch adsorption experiments

The removal of (MGO) dye was investigated under the optimized conditions including the amount of adsorbent, pH, dye concentration, shaking time, ionic strength and temperature. The effect of P^H at point of zero charge, thermodynamic and kinetic studies was also conducted by using Kaolin, Ag-KNC and Ni-KNC nanocomposites.

Effect of dosage of adsorbent

The nanocomposites dosage was diverse from (0.1 to 2.0g)/ 50 mLof MGO dye. The content was shaken at 200rpm at 298K temperature. After the specified time period it was filtered and determines its concentration. The removal efficiency of dye as a function of adsorbent dosage is shown in Fig. 3. It was observed that the adsorption efficiency was enhanced as the adsorbent dose increased from 0.1 to 2.0 g represents the availability of more active sites on the surface of the adsorbent. Consequently it was observed that percentage removal was also improved [35].

Effect of pH

The pH of the system was adjusted from 2-12. Approximately (0.5g) of adsorbent was added in 50mL of the dye solution at specified pH and it was shaken at 200rpm at 298K temperature. The concentration of filtrate after a precise time period was recorded. Fig. 4 indicated that maximum removal efficiency was observed in basic medium. It shows that the basic medium was enriched with OH group provides active sites for the adsorption.

pH at the point of zero charge (PH_{ZPC})

The pH drift method was adopted to investigate the effect of pH at the point of zero charge (pH_{ZPC}) of adsorbents. The pH at which the total number of charges

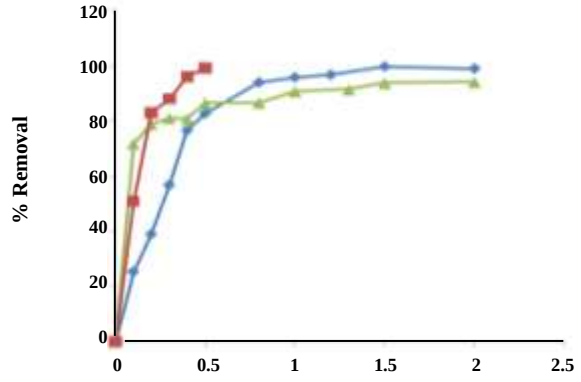

Fig. 3: Optimization of Amount of MGO-kaolin, MGO-Ag-KNC, and MGO-Ni-KNC system.

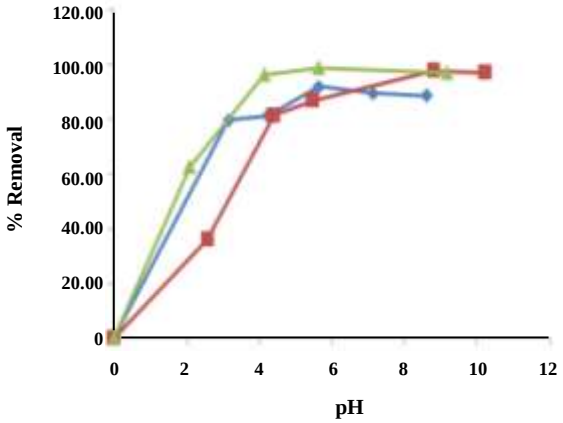

Fig. 4: Optimization of pH of MGO-kaolin,MGO-Ag-KNC and MGO-Ni-KNC system.

on the surface of adsorbent becomes zero is called pH at point zero charge (pH_{ZPC}) [36] .The pH_{ZPC}value of Kaolin, Ag-KNC, and Ni-KNC are shown in Figs. 5 (a - c). They were found to be 6.2, 3.6 and 9.5 for Kaolin, Ag-KNC and Ni-KNC systems respectively.

Effect of shaking time

It was observed that the process of adsorption of MGO was enhanced by the increase in shaking time and removal efficiency was reaches to be an optimum value when the equilibrium between adsorbate and adsorbent was achieved [37]. About 50mL of dye solution was agitated with 0.5g of the adsorbent for variable time intervals at 200 rpm and 298K temperature. The shaking time was varied from 5 to 60 min.

The adsorption capacity of MGO for kaolin was found to be 88.42 % at 30min, for Ag-KNC was 95% at 10min and for Ni-KNC was 92.11% at 60min as shown in Fig. 6.

Electrical Double Layer (EDL) structure

The Electrical Double Layer (EDL) structure of a hydrated particulate was also determined. It represents that an increase in the ionic strength corresponds to an enhancement of EDL. Consequential increase in the adsorption competence was also observed. The thickness of EDL, 1/κ, can be estimated as:

$$\frac{1}{\kappa}=\left(\frac{2F^2\cdot I\cdot 1000}{\varepsilon}\acute{\varepsilon}\cdot RT\right) \quad (1)$$

Where *1/κ* denotes the reciprocal of Debye Length of EDL; F is the Faraday constant (c/mol); *I* is the ionic strength (mol/L); *R* is the molar gas constant (J/mol K); *T* represents the absolute Temperature (K): *ε* stands for the dielectric constant of water and *έ* is the vacuum permittivity(C/(V_m).

The ionic strength also effects on the adsorption of dyes. It shows that the adsorption efficiency was influenced by the concentration of electrolytic species. The presence of KCl electrolyte produces opposing effects in term of adsorption efficiency. Moreover, the electrostatic interaction between dye molecules and adsorbent was observed to be decreased. The increase in decolorization efficiency of MGO facilitates the protonation process [39]. The results are shown in Fig. 7.

Comparative study of adsorption isotherms

There are several isotherm equations describe the adsorption mechanism. The Langmuir, Freundlich, and Dubinin-Radushkevich (D-R) isotherm models were commissioned to fit on experimental data [40].

ADSORPTION STUDIES

Freundlich adsorption isotherms

The empirical equation used to describe the heterogeneous system represent:

$$\mathrm{Log}\frac{X}{m}=\mathrm{Log}K+\frac{1}{n}\mathrm{Log}Ce \quad (2)$$

Where *X/m* is the amount adsorbed per unit mass of the adsorbent, Ce is the equilibrium concentration and 1/n and *K* are Freundlich constants. [41]. The parameter n, is known as the heterogeneity factor, can be used to illustrate whether the adsorption is linear (n=1) a chemical process (nF>1) or a physical process (nF<1).

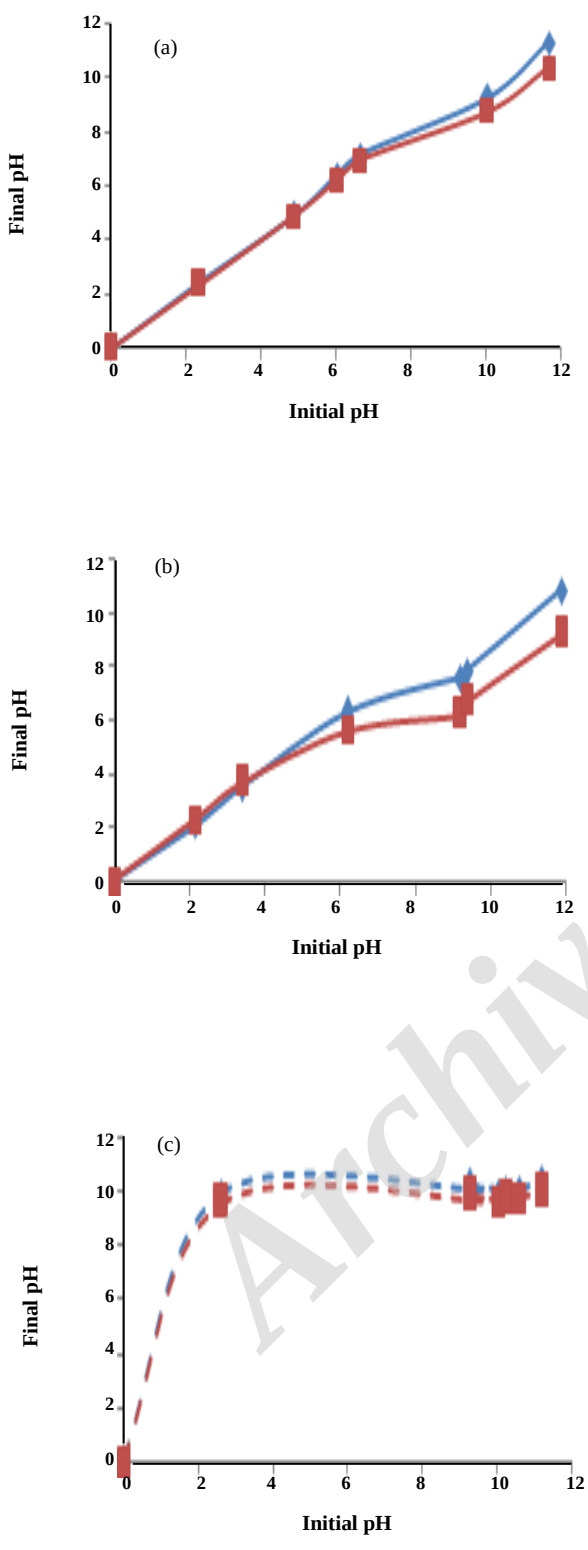

Fig. 5: (a) pH_{ZPC} of kaolin and (b) pH_{ZPC} of Ag-KNC (c) pH_{ZPC} of Ni-KNC.

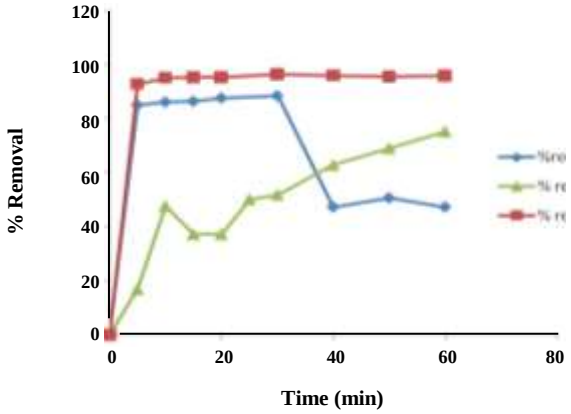

Fig. 6: Optimization of Time of MGO-kaolin, MGO-Ag-KNC and MGO-Ni-KNC system.

In contrast, the values of nF<1 and nF>1 indicate a normal Langmuir isotherm and cooperative adsorption, respectively [33]. The comparative trends at variable temperatures are expressed in Fig. 8.

Langmuir adsorption isotherm

The Langmuir isotherm describes quantitatively the formation of a monolayer of adsorbate on the outer surface of adsorbent and after that no further adsorption takes place. Moreover, it also describes the presence of a finite number of active sites homogeneously distributed over the surface of the adsorbent [42]. The Langmuir isotherm is expressed as

$$\left(\frac{Ce}{X/m}\right)=\left(\frac{1}{KVm}\right)+\left(\frac{Ce}{Vm}\right) \quad (3)$$

The value of K and V_m represent Langmuir constants. The constant K gives a measure of adsorbing capacity and shows the nature of binding and V_m is the monolayer capacity. The comparative trends of respective adsorbents at different temperatures are shown in Fig. 9.

Dubinin Radeshkevish adsorption isotherm

The adsorption data was applied on Dubinin-Radushkevich (D-R) isotherm to estimate the porosity, free energy and the characteristics of adsorbents [34]. The linear form of D–R isotherm is represented as:

$$\mathrm{Ln}\frac{X}{m}=\ln Xm-K\varepsilon^2 \quad (5)$$

Where X_m is the monolayer capacity of adsorbent, K is a constant related to adsorption energy, ε is the mean

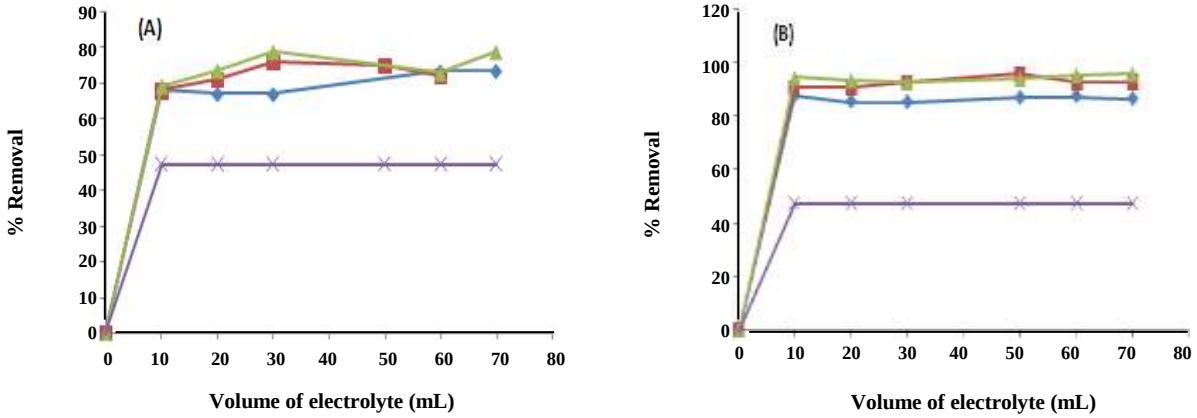

Fig. 7: Effect of ionic strength on (a) MGO-kaolin and (b) MGO-Ni-KNC system.

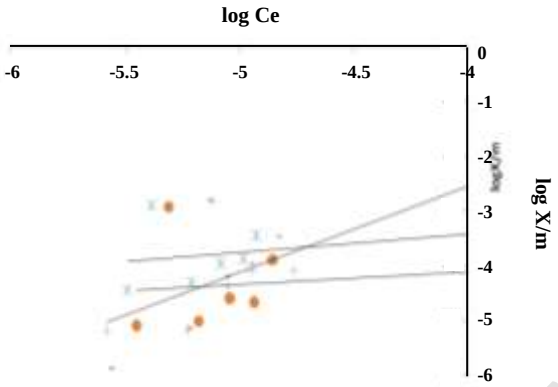

Fig. 8: Freundlich Isotherm of Kaolin, Ag-KNC, and Ni-KNC with MGO system.

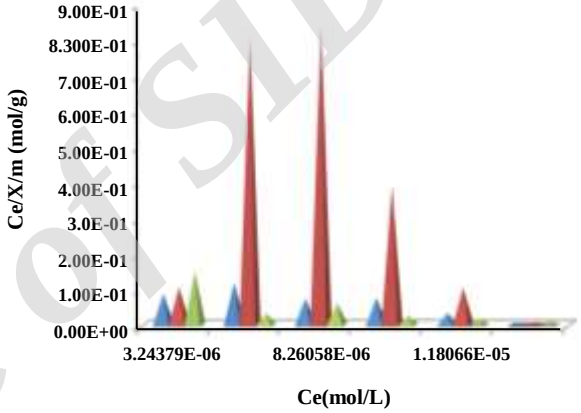

Fig. 9: Comparative Langmuir plots of Kaolin, Ag-KNC, and Ni-KNC with MGO system at 298 K.

free of sorption, which is represented in Eqs. (5) and (6) [43]. In addition, it represents the transfer of one mole of the target from infinity in solution to the surface of the solid. The results are shown in Fig. 10. The comparative study of adsorption isotherm represents that Ag-KNC and Ni-KNC systems show better adsorption capacity compeered to Kaolin. The sorption free energy is calculated as:

$$\varepsilon = RTLn\left(1+\frac{1}{Ce}\right) \qquad (6)$$

The mechanism of adsorption

It was investigated by using Intra-Particle Diffusion (IPD) model and Boyd kinetics model [45 - 47]

Intra-particle diffusion model

The IPD model was proposed by *Weber* and *Morris* and applied for the analysis of adsorption kinetics. There is a functional relationship between the adsorption process and adsorption uptake is almost proportional with $t_{1/2}$ rather than with the contact time (t). The *Weber* and *Morris* Intra particle diffusion model is represented as:

$$\log qt = \log Kid + 0.5\log t \qquad (13)$$

Where the k_{id} is the intra-particle diffusion rate constant, which was obtained from the gradient of the linear plot of log qt vs. t as shown in Fig. 11. The intercept describe the thickness of the boundary layer increases with the proliferation of intercept. The positive values of slope represent the controlled adsorption process.

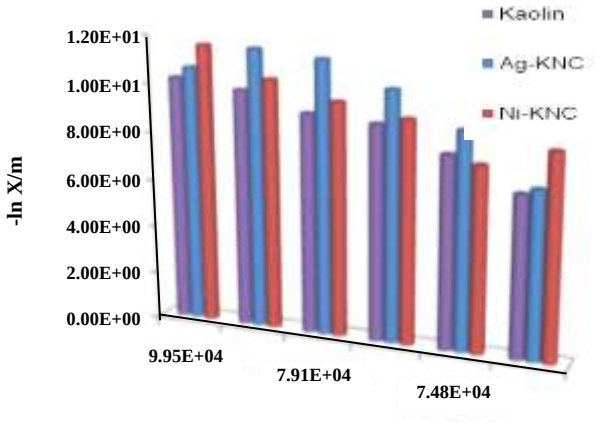

Fig. 10: The Comparative D-R isotherm of Kaolin, Ag-KNC, and Ni-KNC (MGO) system at 298K.

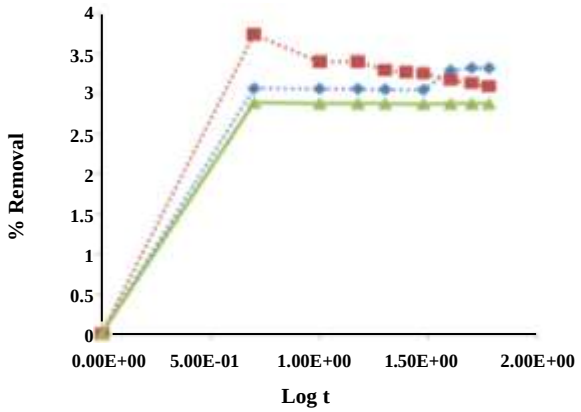

Fig. 11: Intra particle diffusion model of kinetics for Kaolin, Ag-KNC, and Ni-KNC MGO System.

THE BOYD KINETICS MODEL

Boyd's model suggested the slow step adsorption process. It is represented as:

$$F=1-\frac{6}{\pi^2}\exp\left(-B_t\right) \quad (13)$$

$$B_t=-0.4977-\ln\left(1-F\right) \quad (14)$$

The *F* represents the fraction of solute adsorbed on the surface of adsorbent at the time, *t* (min), which is calculated as:

$$F=\frac{qt}{qo} \quad (15)$$

Moreover, three sequential steps can be accomplished from Boyd's model including a film diffusion process, particle diffusion and adsorption of adsorbate. It shows that adsorbate moves towards the surface of the adsorbent and travel within the pores of the adsorbent.

Adsorption kinetic

The rate of adsorption process was determined by Lagergren's pseudo first order and Ho-McKay's pseudo-second order models [44] . They are represented as:

$$\ln\left(q_e-q_t\right)=\ln q_e-k_1t \quad (10)$$

$$\frac{t}{q_t}=\frac{1}{k_2q_e^2}+\frac{t}{q_e} \quad (11)$$

The values of the rate constant and R^2 for the MGO sorption on Kaolin, Ag-KNC and Ni-KNC systems are represented in Fig. 12 and Table 1. The results show that the system follows the pseudo-second-order kinetics.

THERMODYNAMIC PARAMETER

The thermodynamic parameters: ΔG°, ΔH°, and ΔS° were calculated by using the following equations:

$$\ln K_D=\frac{\Delta S^\circ}{R}-\frac{\Delta H^\circ}{RT} \quad (8)$$

$$\Delta G^\circ=\Delta H^\circ-T\Delta S^\circ \quad (9)$$

The values of ΔG° show spontaneous behavior of the system. Moreover, the ΔH° represents exothermic behavior and the values of ΔS° are positive. The results are shown in Tables 2.

CONCLUSIONS

The present investigation showed the synthesis of nanocomposites of Ag-KNC and Ni-KNC by a bottom-up approach. The SEM analysis represents that the nanocomposites have sizes ranging from 50 to 100nm. The enhanced surface area shows higher % removal of MGO dye by nanocomposites compared to Kaolin.

Furthermore, this study provides an efficient methodology for the treatment of textile wastewater. The estimated data was incorporated to determine the rate constant by employing IPD and Ho-McKay's pseudo-second order models. The adsorption data represents that Freundlich isotherm is the best-fitted model. The thermodynamic parameters ΔG^o, ΔH^o and ΔS^o were evaluated, they show spontaneous and exothermic behavior. The surface neutrality of the system was estimated at (pH_{pzc}). Effect of ionic strength on the adsorption of dyes was also estimated in the presence of electrolyte KCl. Moreover, the ionic strength is one

Table 1: Rate constant and Intra-particle-diffusion constant for the adsorption of MGO on Kaolin, Ag-KNC, and Ni-KNC.

Adsorbent	Pseudo-second-order			Intra-particle-diffusion		q_e ,Exp (mg/g)
	k_2 (g/mg.min)	q_e^2,theoretical (g/mg)	R^2	$K_{i.d}$ (g/mg.min)	R^2	
Kaolin	4.30E+02	2.151E-07	0.953	8.542	0.704	2.79E-04
Ni-KNC	7.36E+01	8.47E-07	0.867	22.66	0.455	5.09E-04
Ag-KNC	7.48E+3	1.76E-06	0.996	9.274	0.620	1.33E-03

Table 2: Thermodynamic Parameters for the adsorption of MGO on Kaolin, Ag-KNC, and Ni-KNC at the temperature range 298K-313K.

Adsorbent	Thermodynamic parameters						
	Concentration (ppm)	ΔH^0 (kJ/mol.K)	ΔS^0 (J/mol.K)	ΔG^0 (kJ/mol)			
				298K	303K	308K	313K
KAOLIN	50	-4.775	53.59	-3.724	-3.834	-3.896	-3.971
	100	-3.248	48.68	-3.740	-3.838	-3.904	-3.967
	150	-2.327	45.35	-3.715	-3.832	-3.885	-3.934
	200	-0.485	39.25	-3.717	-3.837	-3.872	-3.919
	300	-2.975	46.75	-3.637	-3.797	-3.884	-3.848
	500	-15.616	79.22	-2.871	-3.045	-3.217	-3.234
Ag-KNC	50	-4.031	24.32	-3.735	-3.818	-3.882	-3.871
	100	-0.188	37.49	-3.777	-3.825	-3.906	-3.959
	150	-0.841	35.34	-3.777	-3.831	-3.898	-3.956
	200	-1.162	34.10	-3.770	-3.815	-3.882	-3.944
	300	- 1.675	31.91	-3.734	-3.774	-3.877	-3.887
	500	-43.153	-111.45	-3.261	-3.496	-3.387	-2.747
Ni-KNC	50	0.176	30.83	-3.298	-3.369	-3.341	-3.491
	100	-15.353	80.85	-3.049	-3.352	-3.374	-3.451
	150	-5.635	49.37	-3.196	-3.358	-3.306	-3.479
	200	-2.0214	102.39	-3.446	-3.774	-3.838	-3.883
	300	-30.811	130.77	-2.818	-3.310	-3.406	-3.442
	500	-42.704	168.63	-2.500	-3.292	-3.421	-3.342

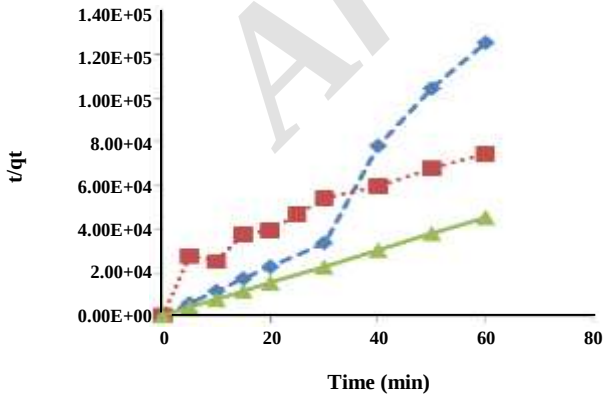

Fig. 12: Pseudo-second order model of kinetics for kaolin, Ag-KNC, and Ni-KNC MGO System.

of the key factors affecting the Electrical Double Layer (EDL) structure of a hydrated particulate.

In the light of current research work, it was concluded that Ag –KNC, and Ni-KNC can be utilized as good adsorbents for the removal of dyes.

CONFLICT OF INTEREST

Author has no conflict of interest regarding the present studies.

Received : May 30, 2016 ; Accepted : Sep. 25, 2017

REFERENCES

[1] Xun W., Jing Z., Qing P.andYadong L., A General Strategy for Nanocrystal Synthesis, *Nature*, **437**: 121-124 (2005).

[2] Balci S., Bittner A.M., Hahn K., Scheu C., Knez M., Kadri A., Wege C., JeskeH.and Kern K., Copper Nanowires within the Central Channel of Tobacco Mosaic Virus Particles, *Electrochimicaacta*, **51**(28): 6251- 6257 (2006).

[3] Meng H., Peng H., Chunlei Z., Feng C., Can W., Jiebing M., Rong H., Daxiang C., A General Strategy for the Synthesis of Upconversion Rare Earth Fluoride Nanocrystalsvia a Novel OA/Ionic Liquid Two-Phase System, *Chemical Communications (Cambridge, England)*, **47**(33): 9510 - 9512 (2011) .

[4] Hajira T., Uroos A., Lignocellulosic: Non-Conventional Low Cost Biosorbent for the Elution of Coomassie Brilliant Blue (R-250), *International Journal of Chemistry*, **6**(2): 56-72(2014).

[5] Nandapure B.I., Kondawar S.B., Salunkhe M.Y., Nandapure A.I., Magnetic And Transport Properties of Conducting polyaniline/nickel Oxide Nanocomposites, *Advanced Materials Letters*, **4**(2): 134-140 (2013).

[6] Ramana G.V., Balaji P., Kumar R.N., PrabhakarK.V., Jain P.K, Mechanical properties of Multi-Walled Carbon Nanotubes Reinforced Polymer Nanocomposites, *Indian journal of Engineering & Material Sciences*, **17**: 331-337 (2010).

[7] Amy M.M., Namiko Y., Matthew A.P., Kenneth E.G., Thermal Conduction in Aligned Carbon Nanotube PolymerNanocomposites with High PackingDensity, *ACS Nano*, **5**(6): 4818-4825 (2011).

[8] Joy K.M., Young W.C., Nak S.C., Preparation and Characterization of Rubber-Toughened poly(trimethylene terephthalate)/ organoclaynanocomposite, *Polymer Engineering & Science*, **47**(6): 863-870 (2007).

[9] Sarika S., Barick K.C., Bahadur D.I., Functional Oxide Nanomaterials and Nanocomposites for the Removal of Heavy Metals and Dyes, *Nanomaterials and Nanotechnology*, **3**(20): 1-19 (2013).

[10] Shameli K., Ahmad M.B., Yunus W.Z., Ibrahim N.A., Darroudi M., Synthesis and Characterization of Silver/Talc Nanocomposites Using the Wet Chemical Reduction Method, *Journal of Nanomedicine*, **5**: 743-751 (2010).

[11] Saeedeh H., Mohammad R.S., Novel Ag/Kaolin Nanocomposite as Adsorbent for Removal of Acid Cyanine 5R from Aqueous Solution, *Journal of Chemistry*, **2013**: 1-7 (2013).

[12] Kamyar S., Mansor B.A., Mohsen Z., Wan M.Z.W.Y., Nor A.I., ParvanehS. and Mansour G.M., Synthesis and Characterization of Silver/montmorillonite/ chitosan Bionanocomposites by Chemical Reduction Method and Their Antibacterial Activity, *Int. J.Nanomedicine*, **6**: 271-284 (2011).

[13] Meshram S., Limaye R., Ghodke S., Nigam S., Sonawane S., Chikate R., Continuous Flow Photocatalytic Reactor Using ZnO–Bentonitenanocomposite for Degradation of Phenol, *Chemical Engineering Journal*, **172**(2): 1008-1015 (2011).

[14] Haghighizadeh A., Tan W.L., Mohammad A.B., Ghani S.A., Synthesis and Properties of Nanosized Silver Catalyst Supported on Chitosan-Silica Nanocomposites, *AIP Conf. Proc.*, **1502**: 255- 271 (2012)

[15] Zhai H.J., Sun D.W., and Wang H.S., Catalytic properties of Silica/Silver Nanocomposites, *Nanoscience Nanotechnology*, **6**(7): 1968 - (2006).

[16] Rapsomanikis A., Papoulis D., Panagiotaras D., Kaplani E., Stathatos E., NanocrystallineTiO_2 and Halloysite Clay Mineral Composite Films Prepared by Sol-Gel Method: Synergistic Effect and the Case of Silver Modification to the Photocatalytic Degradation of Basic Blue- 41 azo Dye in Water, *Global NEST Journal*, **16**: 485-498 (2014).

[17] Nazar H.K., Sirajuddin, Razium A.S., Syed T.H.S., Keith R.H., Abdul R.K., Synthesis and Characterization of Highly Efficient Nickel Nanocatalysts and Their Use in Degradation of Organic Dyes, *International Journal of Metals*, **2014**: 1 - 10 (2014).

[18] Rodiansono R., Takayoshi H., Shogo S., Total Hydrogenation of Biomass-Derived Furfural Over Raney Nickel-Clay Nanocomposite Catalysts, *Indo. J. Chem.*, **13**(2): 101- 107 (2013).

[19] Awwad, A.M., Albiss B.A., Salem N.M., Antibacterial Activity of Synthesized Copper Oxide Nanoparticles Using Malvasylvestris Leaf Extract, *SMU Med. J.*, **2**:91-101 (2015).

[20] Sandipan C., Sudipta C., Bishnu P.C., Arun K.G., Adsorptive Removal of Congo Red, A Carcinogenic Textile Dye by Chitosan Hydrobeads: Binding Mechanism, Equilibrium and Kinetics, *Colloids and Surface A Physicochemical and Engineering Aspects*, **299**: 146-152 (2007).

[21] Jiwan S., Uma, Sushmita B., Yogesh C.S., A Very Fast Removal of Orange G from its Aqueous Solutions by Adsorption on Activated Saw Dust: Kinetic Modeling and Effect of Various Parameters, *International Review of Chemical Engineering*, **4**(1): 1-7 (2012).

[22] Armen B.A., Theory of Global Sustainable Development Based on Microalgae in Bio and Industrial Cycles, Management-Changing Decisions in Areas of Climate Change and Waste Management, *Journal of Sustainable Bioenergy Systems*, **3**(4): 287-297 (2013).

[23] Iqbal M.J., Ashiq M.N., Adsorption of Dyes from Aqueous Solutions on Activated Charcoal, *J. Hazard. Mater*, **139**: 57-66 (2007).

[24] Dotto G.L., Moura J.M., Cadaval T.R.S., Pinto L.A.A., Application of Chitosan Films for the Removal of Food Dyes from Aqueous Solutions by Adsorption, *Chemical Engineering Journal*, **214**: 8-16 (2013).

[25] Debabrata C., Vidya R.P., Anindita S., Moulik S.K., Removal of Some Common Textile Dyes from Aqueous Solution Using Fly Ash, *J. Chem. Eng. Data*, **55**(12): 5653-5657 (2010).

[26] Oladipo O., Randy J.M., Peter W.S., X-Ray Diffraction Study on Highly Ordered Mesostructured Thin Films, JCPDS-International Centre for Diffraction Data, *Advances in X-ray Analysis*, **45**: 359-364 (2002).

[27] Hassan H. Hameed B.H., Fenton-like Oxidation of Acid Red 1 Solutions Using Heterogeneous Catalyst Based on Ball Clay, *International Journal of Environmental Science and Development*, **2**(3): 218-222 (2011).

[28] Saad M., Hajira T., Fakhra S., Synthesis and Characterization of SnO-CoOnanocomposits by Bottom up Approach and Their Efficacy to the Treatment of Dyes Assisted Simulated Waste Water, *Int. J. Curren. Res.*, **7**(12): 23542-23550, (2015).

[29] Meshram S., Limaye R., Ghodke S., Nigam S., Sonawane S., Chikate R., Continuous Flow Photocatalytic Reactor Using ZnO–Bentonitenanocomposite for Degradation of Phenol, *Chemical Engineering Journal*, **172**(2): 1008-1015 , (2011).

[30] George A.K., Insik J., Marit N.H., Ahmed M.A., Jayeeta B., Bharam P., Fluorinated Analogs of Malachite Green: Synthesis and Toxicity, *Molecules*, **13**(4): 986-994 (2008).

[31] Bahareh S., Saeedeh H., Synthesis of Kaolin/Ag Nanocomposite as an Efficient and Versatile Reagent for the Synthesis of 1,8-Dioxo-Octahydroxanthene Derivatives, Synthesis and Reactivity in Inorganic, *Metal-Organic, and Nano-Metal Chemistry*, **44**: 424-428 (2014).

[32] Ghulam M., Hajira T., Muhammad S., Nasir A., Synthesis and Characterization of Cupric Oxide (CuO) Nanoparticles and Their Application for the Removal of Dyes, **12**(47): 6650-6660 (2013).

[33] Mantosh K.S., Priya B., Papita D.J., Plant-Mediated Synthesis of Silver-Nanocomposite as Novel Effective Azo Dye Adsorbent, *Applied Nanoscience*, *doi:10.1007/s13204-013-0286-x* (2013).

[34] Hajira T., Muhammad S., Zainab Q., Physiochemical Modification and Characterization of Bentonite Clay and Its Application for the Removal of Reactive Dyes, *International Journal of Chemistry*, **5**(3): 19- 32 (2013).

[35] Venkateswaran V., Priya T., Equilibrium and Kinetics of Adsorption of Cationic Dyes by STISHOVITE-Clay –TiO_2 Nanocomposite, *Intrenational Journal of Modern Engineering Research (IJMER)*, **2**(6): 3989-3995 (2012).

[36] Gholam R.M., Roghaye Z.J., Removal Kinetic of Cationic Dye Using Poly (Sodium Acrylate)-Carrageenan/Na-Montmorillonite Nanocomposite Superabsorbents, *Mater. Environ. Sci.*, **3**(5): 895-906 (2012).

[37] Saad M., Hajira T., Khan J., Hameed U., Saud A., Synthesis of Polyaniline nanoparticles and their application for the removal of Crystal Violet dye by Ultrasonicated adsorption Process Based on Response Surface Methodology, *Ultrasonic. Sonochem.*, **34**: 600-608 (2017).

[38] Samarghandi M.R., Zarabi M., Noori Sepehr M., Panahi R., Foroghi M., Removal of Acid Red 14 by Pumice Stone as a Low Cost Adsorbent: Kinetic and Equilibrium Study, *Iranian Journal of Chemistry & Chemical Engineering (IJCCE)*, **31**(3): 19-27 (2012).

[39] Yao-Jen T., Chen-Feng Y., Chien-Kuei C.J., Kinetics and Thermodynamics of Adsorption for Cd on Green Manufactured Nano-Particles, *Hazard Mater.*, **235-236**: 116-122 (2012).

[40] Mokhtari P., Ghaedi M., Dashtian K., Rahimi M.R., Purkait M.K., Removal of Methyl Orange by Copper Sulfide Nanoparticles Loaded Activated Carbon: Kinetic and Isotherm Investigation, *Journal of Molecular*, **219**: 299-305 (2016).

[41] Vijayakumar G., Tamilarasan R., Dharmendirakumar M.J., Adsorption, Kinetic, Equilibrium and Thermodynamic Studies on the Removal of Basic Dye Rhodamine-B from Aqueous Solution by the Use of Natural Adsorbent Perlite, *Mater. Environ. Sci.*, **3**(1): 157-170 (2012)

[42] Saad M., Hajira T., Synthesis of Carbon Loaded γ-Fe_2O_3Nanocomposite and Their Applicability for the Selective Removal Of Binary Mixture of Dyes by Ultrasonic Adsorption Based on Response Surface Methodology, *Ultrasonic. Sonochemis.*, **36**: 393-408 (2017).

[43] Kamali M., Ghorashi S.A.A., Asadollahi M.A., Controllable Synthesis of Silver Nanoparticles Using Citrate as Complexing Agent: Characterization of Nanopartciles and Effect of pH on Size and Crystallinity, *Iranian Journal of Chemistry and Chemical Engineering (IJCCE)*, **31**(4): 21-28 (2012).

[44] Okewale A.O., Babayemi K.A., Olalekan A.P., Adsorption Isotherms and Kinetics Models of Starchy Adsorbents on Uptake of Water from Ethanol – Water Systems, *International Journal of Applied Science and Technology*, **3**(1): 35-42 (2013).

[45] Naghizadeh A., Ghafouri M., Synthesis and Performance Evaluation of Chitosan Prepared from Persian Gulf Shrimp Shell in Removal of Reactive Blue 29 Dye from Aqueous Solution (Isotherm, Thermodynamic and Kinetic Study), *Iranian Journal of Chemistry and Chemical Engineering (IJCCE)*, **36**(3): 25-36 (2017).

[46] Hameed B.H., Mohd-Din A.T., Ahmad A.L., Adsorption of Methylene Blue onto Bamboo-Based Activated Carbon: Kinetics and Equilibrium Studies, *Journal of Hazardous Materials*, **141**(3): 819-825 (2007).

[47] Esmaeili A., Ghasemi S., Zamani F., Investigation of Cr(VI) Adsorption by Dried Brown Algae Sargassum sp. and Its Activated Carbon, *Iranian Journal of Chemistry and Chemical Engineering (IJCCE)*, **31**(4): 11-19 (2012).